


INTERFACIAL MICROSTRUCTURE FORMATION IN Al7SiMg/Cu COMPOUND CASTINGS

Aina Opsal Bakke , Lars Arnberg, and Yanjun Li

Department of Materials Science and Engineering, Norwegian University of Science and Technology, Alfred Getz' vei 2, 7034 Trondheim, Norway

Jan-Ove Løland, Svein Jørgensen, and Jan Kvinge

Aludyne Norway, Vollmonaveien 7, 4550 Farsund, Norway

Copyright © 2020 The Author(s)

<https://doi.org/10.1007/s40962-020-00463-w>

Abstract

Compound casting is an attractive approach to create multi-material components and thus reduce the overall weight, while maintaining both the functional and mechanical properties. In this work, Al7SiMg alloy/copper compound castings were produced by a low-pressure die casting process. A flux coating was applied on copper pipes to reduce the oxide layer present in the interface between Al and Cu. The interface layer formed between the two alloys was investigated using optical microscopy, scanning electron microscopy and energy-dispersive X-ray spectroscopy. Vickers micro-hardness was also measured across the interface. Results showed that a continuous metallurgical bond formed between copper and aluminum without use of surface treatment. In the bond layer, various

Al–Cu intermetallic phases were detected, as well as primary silicon particles and the quaternary phase $Al_5Cu_2Mg_8Si_6$. Flux coating prevented formation of any metallic bond between copper and aluminum. Instead, high concentrations of potassium, magnesium and fluorine, indicative of formation of $KMgF_3$ and MgF_2 , were detected in the interface. The mechanism for the formation of the intermetallic phases and the strength of the interface layer have been discussed.

Keywords: aluminum alloys, compound casting, flux coating, microstructure

Introduction

Recent development in the automotive industry has focused on lightweight components, which can reduce CO₂ emission. Often, one material alone is not able to meet the requirements for a specific application. The need for lightweight bimetallic components has therefore increased. Aluminum–copper bimetallic components can be used in wires and bus bars where conductivity is an important factor.¹ Compared to Al–Cu alloys, Al–Cu bimetallic components can reduce both weight and cost without reducing electrical and thermal conductivity.² A challenge is, however, that aluminum and copper have high affinity to each other, especially at elevated temperatures. This causes formation of brittle intermetallic phases with high electric resistance.³ More importantly, both metals are subjected to oxide formation on the surface. While copper is exposed to oxidation at elevated temperatures,⁴ a stable and

passivating oxide layer will spontaneously form on the aluminum melt surface during casting.⁵ Oxides are known to reduce wettability and will thus prevent formation of a metallurgical bond between aluminum and copper.⁶

Different approaches have been used to join aluminum and copper, such as friction stir welding,^{7,8} cold roll bonding,⁹ explosive welding¹⁰ and diffusion bonding.¹¹ Although metallurgical bonds can form between the two materials by these methods, they often require long process time and have specific geometrical restrictions, making them less cost-effective for massive industrial production.¹²

Compound casting is a method of joining two metals: one in solid and one in liquid state. The solid material is pre-inserted in the mold with the liquid subsequently being cast around it. A diffusion layer will form between the two materials, generating continuous metallurgical bonding.¹³

Published online: 06 May 2020

A similar process, named composite casting or discontinuous compound casting, has gained much attention. In this process, a metal is first cast into the mold. Then, when this metal has reached a certain temperature, $T_{\text{Substrate}}$, the second metal is cast onto it.^{14–16} These processes allow production of complex geometries, as well as reducing the process time due to the direct insertion of the solid material or the casting of the first material. This increases the process efficiency and lowers cost.¹⁷

Several investigations on the interfacial reaction layer forming during joining of aluminum and copper through a compound casting process have been presented. In general, the reaction layer shows formation of Al_4Cu_9 , Al_3Cu_4 , AlCu , Al_2Cu and $\text{Al}_2\text{Cu} + \text{Al}$ eutectic from the copper side to the aluminum side consequently.¹⁸ However, different process parameters prevent some of the phases from forming. Chu et al. reported formation of an Al_4Cu_9 layer at the interface followed by an Al_2Cu layer with acicular $\text{Cu}_3\text{Al}_{2+x}$ embedded, after a core-filling continuous casting process with 99.9% Cu and Al.¹⁹ Su et al. showed that an increase in the Al casting temperature caused an increased thickness of the $\text{Al}_2\text{Cu} + \text{Al}$ eutectic layer, whereas the Al_4Cu_9 and Al_2Cu phases decreased.²⁰ Similar discoveries were made by Pintore et al., who found that a higher substrate temperature caused a thicker reaction layer, especially of the eutectic $\text{Al}_2\text{Cu} + \text{Al}$. They also observed that a Cu substrate below 400 °C caused cracks in the interface and poor bonding.²¹

Both Jiang et al.²² and Divandari and Golpayegani²³ studied the Al A356 (7 wt% Si)–Cu interface after a lost foam casting (LFC) process. In this process, a copper insert was placed in a polystyrene pattern, which then burns when the molten aluminum is poured into the mold. Results showed that in addition to the $\text{Al}_2\text{Cu} + \text{Al}$ eutectic and the Al–Cu phases at the copper surface, silicon particles formed in the reaction layer. It was also observed that the LFC process caused a large area of the Cu insert to melt during the casting, with Divandari and Golpayegani reporting complete melting of a Cu wire with 0.4 mm diameter.

The study of Zare et al.²⁴ on Al/Cu compound casting showed that metallurgical bonding with formation of intermetallic phases only formed locally at the interface. A large fraction of the interface areas showed gaps due to the oxide film forming on the aluminum melt surface. It was

concluded that as the melt is poured, shear stress from the melt convection would be able to remove oxides in certain areas, which resulted in metal–metal contact and metallurgical bonding. To reduce oxides on the copper surface, Liu et al. used thermal spray coating of zinc on the copper pipes. This resulted in a continuous metallurgical bond at the interface. The intermetallic phases formed at the interface were identified as Al_4Cu_9 and Al_2Cu . 700 °C was deemed preferable pouring temperature as lower temperatures caused segregation of zinc in the interface, while a higher temperature resulted in a thicker intermetallic layer.³

The present research focuses on the formation and characterization of the interface between an Al7SiMg alloy and commercially pure copper through a low-pressure die casting process. The metal flow in low-pressure die casting differs from that of gravity casting, which can affect the reaction between aluminum and copper. Differences in the interfacial Al–Cu reaction layer based on alloying elements in the aluminum alloy have been discussed. In addition, the possibility of reducing surface oxides was tested by applying a flux coating on the copper pipes prior to casting. The effect of the flux coating on bonding and formation of intermetallic phases was investigated by optical and electron microscopy.

Materials and Methods

Bimetallic Al/Cu compound castings were produced through a low-pressure die casting process, known as vacuum/pressure riserless casting (VRC/PRC), using commercially pure copper (99.9%) and aluminum alloy A356. The chemical composition of the experimental A356 alloy is presented in Table 1.

Aludyne Norway conducted the casting at their facilities. Copper pipes with diameter of 10 mm and 0.8 mm wall thickness were used. The pipes were thoroughly cleaned with ethanol prior to casting. Flux coating was applied to some of the copper inserts. NOCOLOK® Cs Flux, which is a mixture of $\text{K}_{1-3}\text{AlF}_{3-6}$ and CsAlF_4 , was mixed with denatured alcohol to an alcohol/flux ratio of approximately 7.9. The mixture was then applied to the copper pipes using a small paint brush. The flux has a melting range of 558–566 °C.²⁵ Both the flux-coated and uncoated copper pipes were pre-heated to approximately 200 °C before they

Table 1. Chemical Composition of Aluminum Alloy A356

	Composition (wt%)								
	Si	Mg	Ti	Fe	Sr	Ga	Zn	Others	Al
A356.0	7.0	0.41	0.11	0.082	0.013	0.0089	0.0042	0.0029	Bal.

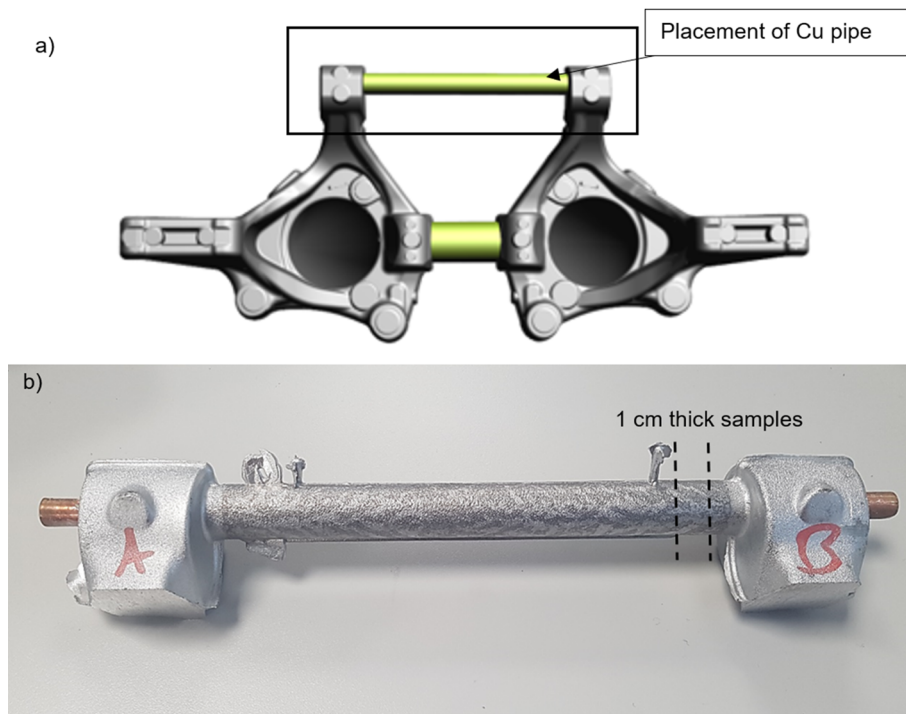


Figure 1. (a) Model of the Al/Cu compound casting. The copper pipe is placed in the upper yellow section. (b) Picture of the casting within the black rectangle in (a) with the specification of the sample cutting pattern after casting. The copper pipe can be seen going through the section.

were placed in a steel mold. Figure 1a shows a model of the finished compound casting. The copper pipes were placed in the upper yellow section shown in the figure. An image of the casting within the black rectangle in Figure 1a can be seen in Figure 1b. The edges of the copper pipe can also be seen in this figure. Four thermocouples were placed in the bottom mold and six in the top mold to control the temperature throughout the casting process. Liquid A356 was received from the smelter at a temperature of 750 °C. After degassing, the melt was poured into the mold. The pouring temperature was in the range of 712–714 °C. During the casting process, the mold remains at a temperature of 300–375 °C and the melt between 680 and 690 °C. Pressure is added stepwise, starting at 0.5 psig, then increasing to 1.8 and 3.0 psig before finally dropping to 0.5 psig. The mold has a water-cooling system that helps control the solidification sequence and cooling rate of the castings. Out of the castings, four representative casting samples that showed the general trend of the castings with similar surface treatment were chosen. Castings A and B have identical casting parameters and are examples of compound castings where the copper pipe had no surface treatment prior to casting. Castings C and D have the same casting process parameters as A and B, but for these castings, the copper pipe was coated with the NOCO-LOK® Cs Flux prior to casting.

After casting, cross section samples with approximately 1 cm thickness were cut from the castings as shown in

Figure 1b. The samples were ground to 4000 grits using a Struers LaboPol-21, followed by polishing using 3 μm and 1 μm diamond suspension on a Struers Tegramin-20. The aluminum–copper interface and potential reaction zone were investigated in a Leica MEF4M optical microscope. Further characterization of the interface was done in a Zeiss Supra 55VP Field Emission Scanning Electron Microscope (FESEM). Working distance was set to 10 mm and acceleration voltage to 15 kV. To identify observed phases in the interface, energy-dispersive X-ray spectroscopy (EDS) was used. Vickers micro-hardness was measured across the interface of each sample using a Leica VMHT MOT micro-hardness tester with 25 g load and 10 s holding time.

Results

Effect of Surface Treatment

In the interface of castings A and B, without surface coating, no defects could be observed by visual examination, while small cavities were observed in the interface in the flux-coated castings C and D. A closer examination of the A356/Cu interface in casting B, by optical microscopy, is shown in Figure 2a. A reaction zone, indicated by a dotted line, with relatively uniform thickness and only a few small gaps, can be observed. The slight color variation in the reaction zone suggests formation of intermetallic

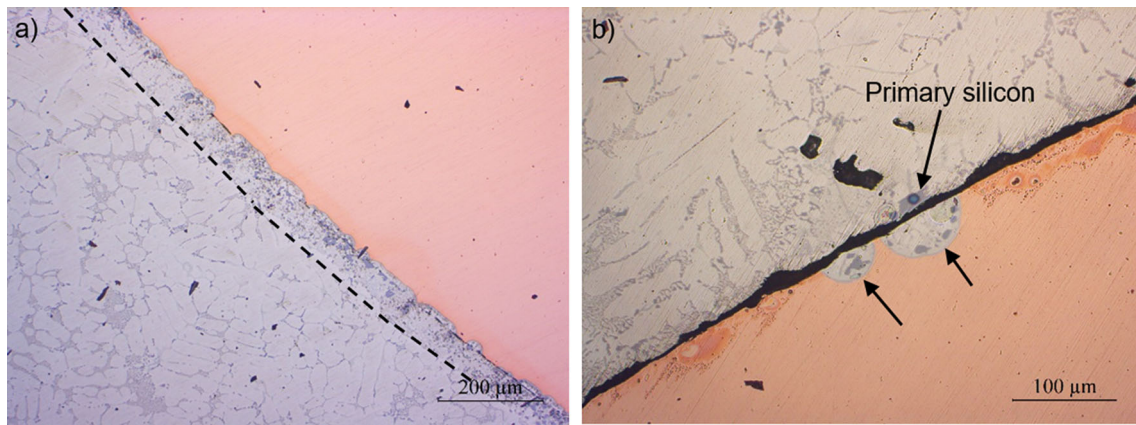


Figure 2. Optical micrograph of the A356/Cu interface in (a) casting B, without surface treatment, where the reaction zone is indicated by the dotted line, (b) casting C, with flux coating.

phases. Casting A also showed local areas of continuous metallurgical bonding, although the reaction areas were less uniform and instead showed an irregular wavy shape at the copper surface.

In both flux-coated castings, instead of a continuous reaction layer as seen in the uncoated samples, large gaps were observed between the copper pipe and the cast A356. The gap has an average width of 8 μm for casting C and 18 μm for D. Figure 2b shows an optical micrograph of the interface structure in casting C. Interestingly, small aluminum-rich features with a droplet-like shape can be observed on the copper side of the interface, as indicated by the arrows. This implies that aluminum melt has dissolved local areas of the copper pipe surface, which differs from the interfaces observed in castings A and B where large continuous reaction layers were observed. This difference between the flux-coated and uncoated copper pipes should be due to the poor wettability between the aluminum melt and the copper pipe in the latter case. In the optical micrograph, it can be seen that the structure in these areas differs from the Al–Si eutectic structure observed in

the cast aluminum. This suggests formation of intermetallic phases within these areas.

Microstructure Characterization

Figure 3 shows a backscattered electron (BSE) image of the interface in casting B. Similar observations could be made for casting A. As can be seen, there is a continuous interface layer composed of a eutectic structure, with approximately 70 μm thickness. Table 2 shows the measured chemical compositions of the representative phases in the interface layer. Most of the irregular bright grey phase is determined as Al_2Cu (Area 2 in Figure 3). In addition to the Al_2Cu eutectic phase, a dark grey phase (Area 1) can be observed. This is likely Q-phase, which is a quaternary phase with the chemical composition $\text{Al}_5\text{Cu}_2\text{Mg}_8\text{Si}_6$. The measured concentrations of Cu, Mg and Si in the Q-phase are lower than the ideal stoichiometric composition, which is due to the small size of the phase and that a large fraction of Al matrix was included in the EDS measurement. Among the eutectic structure, dark grey particles (Area 3) can also be observed, which is presumed to be primary Si. There is also a layer of a plate-shaped phase in close connection with the Cu surface (Area 4)

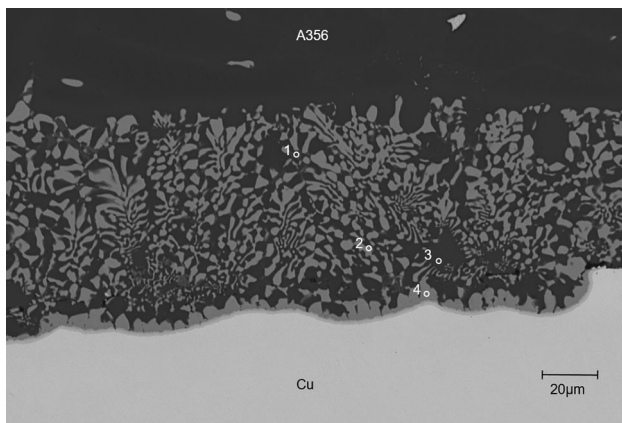


Figure 3. Micrograph of the reaction zone formed in the A356/Cu interface in casting B.

Table 2. Compositions and Possible Phases Detected Through the EDS Analysis of the A356/Cu Interface in Casting B

Area	Composition (at%)				Possible phase
	Al	Cu	Si	Mg	
1	53.31	2.10	5.07	4.98	Q-phase
2	71.58	28.42	–	–	Al_2Cu
3	1.74	0.71	97.55	–	Primary Si
4	69.55	30.45	–	–	Al_2Cu

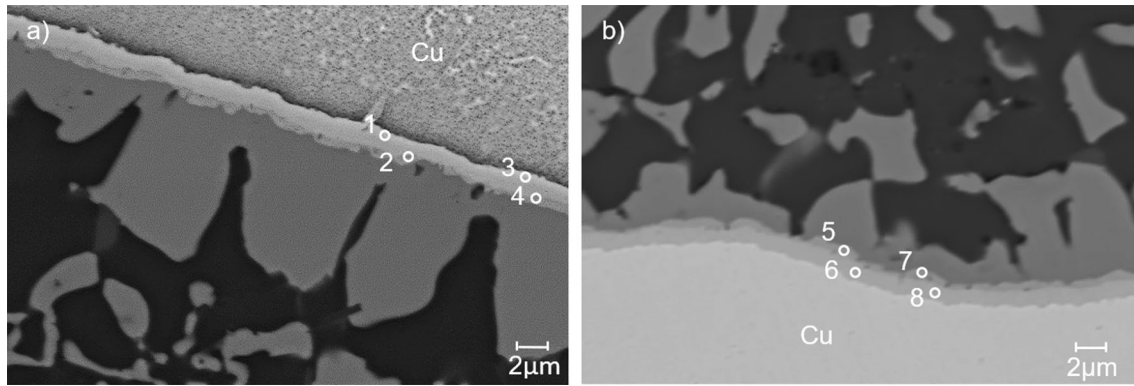


Figure 4. Micrographs of the A356/Cu interface at the copper surface of casting: (a) A, (b) B.

4), which has similar chemical composition as the irregular Al_2Cu eutectic phase.

Figure 4 shows typical microstructures of the A356/Cu interface at the copper surface in castings A and B. As backscattered electrons were used for the micrograph, the contrast difference in the interface suggests formation of two intermetallic phases differing from Al_2Cu . It is, however, difficult to identify the two phases. In casting A, as indicated by the EDS measurements in Table 3, the intermetallic phase closest to the copper pipe (Areas 1 and 3 in Figure 4a) is suggested to be Al_4Cu_9 , while the second layer of intermetallic phase could be either AlCu or Al_2Cu_3 (Areas 2 and 4). It is possible that both have formed in the interface due to the varying local concentration of dissolved copper in the A356 melt. In casting B, the intermetallic phase adjacent to the copper surface is likely Al_2Cu_3 , while the second layer could be AlCu . These results show that different copper-rich Al–Cu intermetallic phases formed at the interface in the compound castings, despite the casting parameters being identical.

Figure 5a shows a BSE image of the reaction area, with droplet-like shape, at the interface of casting C, while

Table 3. Compositions and Possible Phases Detected Through the EDS Analysis of the A356/Cu Interface at the Copper Surface in Castings A and B

Area	Composition (at%)				Possible phase
	Cu	Si	O		
1	12.61	78.23	–	9.16	Al_4Cu_9
2	39.87	60.13	–	–	Al_2Cu_3
3	27.48	64.97	–	7.55	Al_4Cu_9
4	49.17	46.78	1.43	2.61	AlCu
5	54.43	45.57	–	–	AlCu
6	37.40	62.60	–	–	Al_2Cu_3
7	64.83	31.41	1.21	2.55	Al_2Cu
8	40.45	59.55	–	–	Al_2Cu_3

Table 4 presents the chemical compositions of the labeled features measured by EDS. As can be seen, there is a continuous light grey layer at the copper surface in the reaction area (Area 1). This is determined to be the Al_2Cu_3 phase. In connection with the Al_2Cu_3 layer, there is a thicker but less continuous intermetallic phase layer, which is determined as the Al_2Cu phase (Area 2). These two layers follow the outline of the reaction area and distinguish the local area where copper has been dissolved. Inside the reaction area, the irregular-shaped grey phase is determined to be the eutectic $\text{Al}_2\text{Cu} + (\text{Al})$ phase (Area 4). Primary Si particles were also detected among the eutectic phase (Area 3), although these dark particles are difficult to distinguish in the image due to the contrast being similar to the aluminum matrix. The formation of the reaction area is attributed to local melting of the Cu surface during casting. This is evident from the irregular $\text{Al}_2\text{Cu} + (\text{Al})$ eutectic phase found on the aluminum side (Area 7). Thus, formation of the droplet solidification microstructures at the interface in casting C is based on the same mechanism as that of the continuous interface layer in casting B.

It can also be seen that the gap observed in the optical micrograph in Figure 2b is not as wide as initially suggested. Instead, a discontinuous structure can be observed in most of the gap. From the analysis in Area 5, high concentrations of potassium, magnesium and fluorine were detected in this area, indicating that this is a residue from the coating layer. In casting D, shown in Figure 5b, the EDS analysis shows that no Al–Cu intermetallic phases have formed, although the detection of copper in all analyzed areas indicates that a reaction has occurred. Detection of potassium, magnesium and fluorine (Areas 2 and 3) suggests formation of KMgF_3 in the interface. The magnesium concentrations detected in the interface layers of castings C and D significantly exceed the nominal magnesium concentration in the A356 alloy.

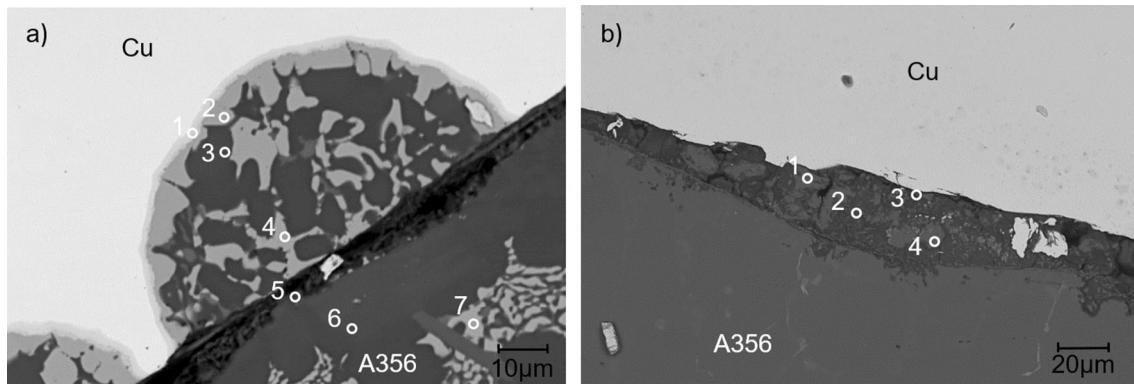


Figure 5. Micrographs of the reaction area formed in the A356/Cu interface in casting: (a) C, (b) D.

Table 4. Compositions and Possible Phases Detected Through the EDS Analysis of the A356/Cu Interface in Castings C and D

Casting area	Composition (at%)							Possible phase
	Al	Cu	Si	Mg	K	F	O	
C-1	37.17	62.83	–	–	–	–	–	Al ₂ Cu ₃
C-2	69.18	30.82	–	–	–	–	–	Al ₂ Cu
C-3	1.14	0.82	98.04	–	–	–	–	Primary Si
C-4	70.17	29.83	–	–	–	–	–	Al ₂ Cu
C-5	36.39	16.48	3.71	10.53	6.90	25.98	–	Flux residue + MgF ₂
C-6	2.30	–	97.70	–	–	–	–	Primary Si
C-7	70.34	28.30	1.37	–	–	–	–	Al ₂ Cu
D-1	97.26	–	2.74	–	–	–	–	(Al)
D-2	27.44	0.70	2.98	2.69	3.70	20.01	42.49	KMgF ₃ + (Al)
D-3	17.09	7.18	–	–	11.61	9.22	54.91	Flux residue
D-4	64.29	1.37	22.15	–	–	–	–	(Al) + (Si)

Micro-hardness Across the Al/Cu Interface

Vickers hardness was measured across the A356/Cu interface for the castings. Figure 6 shows the areas where hardness was measured and the corresponding hardness profiles. Zero in the graph is defined as the interface between the Cu pipe and the reaction layer (Al₄Cu₉, Al₂Cu₃ or AlCu depending on the casting). In all castings, there was a hardness peak in the interface, although the indentations seen are too large to determine the hardness for each separate phase. In comparison with the copper pipe and cast A356 alloy, the hardness in the interface has approximately doubled. This is due to the solution hardening of Cu in Al and strengthening by the hard Al–Cu intermetallic phases. However, the Al–Cu phases are known to be brittle, which might also cause cracks in the reaction layer. A slightly wider area of high hardness can be observed in the flux-coated casting, which coincides with the larger droplet-shaped reaction area formed in this casting.

In Figure 6b and c, cracks can be observed in the reaction layer. As previously mentioned, for the flux-coated castings these areas with cracks were found to have MgF₂, KMgF₃

and flux residue, which hinder the formation of metallic bonding and also act as initiation source for cracks during cooling. For the castings without surface treatment, shown in Figure 6b, the cracks can be observed going through the reaction layer, which suggests that the cracks occur upon solidification. As large concentrations of Si particles are observed adjacent to the cracks, it is believed that these particles could also induce stress concentration resulting in cracks during solidification. In some areas, however, a gap can be observed directly between the copper pipe and cast aluminum. As no reaction has occurred in these areas, it is likely that they remain due to the surface oxides on A356 and copper preventing a reaction between the two.

Discussion

Formation of Interfacial Metallic Bond Layer

All interface layers in the castings showed similar microstructure as previously reported: the eutectic Al₂Cu + (Al) phase dominates, whereas more copper-rich

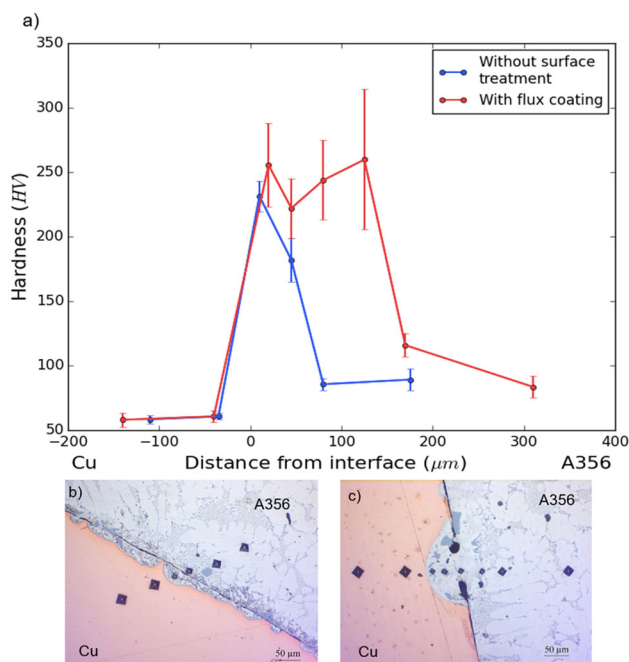


Figure 6. Vickers micro-hardness measured across the Cu/A356 reaction layer in the compound castings. Zero is defined as the interface between the Cu pipe and the reaction layer. (a) Vickers hardness measured for each indentation, (b) indentations across casting B, without surface treatment flux coating, (c) indentations across casting B, with flux coating.

intermetallic phases form adjacent to the copper insert/substrate.^{21,26} However, not all intermetallic phases in the Al–Cu system were observed in the reaction layers. This was more evident for the flux-coated castings, where small reaction areas formed and only the copper-rich Al_2Cu_3 phase was detected. Tavassoli et al. suggested that more copper-rich phases form between Al_2Cu and Cu through solid-state phase transformation once the temperature drops below the eutectic temperature.²⁷ This could explain why not all phases were observed in the reaction areas, as there might be slight differences in the copper pipe surface prior to casting as well as local temperature variations during casting that results in various dissolutions of copper and degree of solid-state phase transformation. A higher temperature will allow more copper to dissolve in the aluminum melt, forming a thicker interfacial bonding layer. Therefore, an optimization of the pre-heating temperature of the copper insert is important in order to improve the bonding layer in terms of thickness and microstructure. In addition to the copper-rich binary phases, the quaternary $\text{Al}_5\text{Cu}_2\text{Mg}_8\text{Si}_6$ phase was detected adjacent to the eutectic Al_2Cu . Zheng et al. reported that a high Cu/Mg ratio would promote formation of the Q-phase,²⁸ while Samuel observed thick plates of $\text{Al}_5\text{Cu}_2\text{Mg}_8\text{Si}_6$ growing from the Al_2Cu during solution treatment of an Al–Si–Cu alloy with 0.45 wt.% Mg.²⁹ When copper dissolves in the A356 alloy, the Cu/Mg ratio will be very high and can thus promote the formation of the

Q-phase from the $\text{Al}_2\text{Cu} + (\text{Al})$ eutectic during solidification.

Primary silicon particles have previously been reported to form among the $\text{Al}_2\text{Cu} + (\text{Al})$ eutectic and at the A356/Cu interface.^{22,23} It was suggested that the formation of these particles was a result of the increased cooling effect induced by copper as some of the particles were formed without melting of the copper insert. It is known that copper has a much higher heat capacity than aluminum, which would increase the cooling rate of A356 at the copper surface. This could cause an undercooling effect and thus promote nucleation of primary silicon. However, in both literature^{22,23} and the present work, primary silicon particles are also observed in between the $\text{Al}_2\text{Cu} + (\text{Al})$ eutectic with some distance to the copper surface. In addition, no silicon particles can be observed outside the reaction areas for the flux-coated castings in this work. This would imply that a dissolution of copper in the aluminum melt is necessary for the formation of primary silicon particles. Most copper pipes are made of phosphorous deoxidized copper, which usually have a residual impurity of approximately 0.01–0.03% phosphorous.³⁰ When the copper pipe is dissolved in liquid A356, AIP will form due to the extremely low solubility of phosphorous in the aluminum melt. It has been reported that as little as 2 ppm phosphorous in the melt is sufficient to form AIP, which can work as heterogeneous nucleation sites for silicon.³¹ This allows primary Si to form above the Al–Si eutectic temperature and can explain why the primary silicon particles only formed in the reaction region.

Effect of Flux Coating

Reaction areas formed in both the flux-coated and uncoated castings, although very limited in the flux-coated ones. Copper has a melting point of 1085 °C,³² which is well above the pouring temperature of the liquid A356. However, according to the binary Al–Cu phase diagram, at the eutectic temperature of 548 °C copper has a solubility of approximately 5.5 wt% in aluminum.³³ During casting, the high-temperature aluminum liquid will react with the copper pipe surface. The variation in reaction area location and size is believed to be a result of variations in the local temperature of the copper surface. When copper dissolves in the aluminum, it leads to a high copper concentration in the aluminum melt locally around the interface. During solidification, a large fraction of Al–Cu intermetallic phases form at the interface. It is likely that the cracks in the interface layer have formed after solidification. Aluminum shrinks upon solidification, causing a buildup of internal stress in the casting. In combination with a high concentration of brittle Al–Cu phases as well as large primary Si particles, cracking might occur. Although gaps are visible in all castings, there is a significant difference in the uncoated and flux-coated ones. In the flux-coated castings,

the gaps are continuous with barely any reaction areas. This suggests that the flux has prevented dissolution of copper and thus also formation of a continuous metallurgical bond.

K_xAlF_y fluxes are often used in aluminum brazing to reduce the aluminum oxide layer. Takemoto et al. reported that magnesium is highly reactive toward such fluxes.³⁴ Magnesium in the aluminum liquid will therefore diffuse to the surface and react with the flux, creating compounds such as MgF_2 and $KMgF_3$. Both these phases have higher melting points than the flux.³² The process temperatures will not melt the flux properly and would therefore reduce its efficiency. The unmelted flux layer on the copper pipes will decrease the wettability between aluminum and copper and prevent the removal of surface oxides, resulting in poor bonding. Garcia et al. however, reported that an addition of 2.0% Cs to the flux would prevent formation of these detrimental magnesium compounds.³⁵ Instead, magnesium will react with cesium and form compounds that have lower melting points and thus do not interfere with the flux. NOCOLOK® Cs flux has a minimum of 1.5% cesium,²⁵ which should be sufficient to prevent formation of MgF_2 and $KMgF_3$. However, as they were detected in these interfaces, the flux has not provided proper wetting between copper and aluminum A356.

Conclusions

From the present research, the following conclusions can be drawn:

Metallurgical bonding between A356 aluminum and the Cu insert was achieved through a low-pressure die casting process without surface treatment of the copper inserts. A reaction layer was observed in all casting samples. The layer mainly consisted of a eutectic $Al_2Cu + (Al)$ structure in addition to a variety of binary Al–Cu compounds such as Al_2Cu , $AlCu$, Al_4Cu_9 and Al_2Cu_3 .

Large primary silicon particles and the quaternary Q-phase $Al_5Cu_2Mg_8Si_6$ also formed in the Al–Cu reaction layer. Silicon particles were believed to nucleate on AlP particles forming when copper dissolved in aluminum, whereas the Q-phase likely formed due to the high Cu/Mg ratio in the reaction layer.

Flux coating of the copper pipes caused formation of magnesium-rich compounds, such as MgF_2 and $KMgF_3$, with higher melting temperatures than the flux. These compounds prevent surface oxide removal of both the copper and aluminum and therefore decrease wettability.

Micro-hardness measurements showed a significant increase in hardness around the reaction layer, which is due

to the solid solution strengthening effect of Cu in Al and the strengthening by hard Al–Cu intermetallic phases.

Acknowledgements

Open Access funding provided by NTNU Norwegian University of Science and Technology (incl St. Olavs Hospital - Trondheim University Hospital). The authors are grateful for the Research Council of Norway for financial support through the IPN Project “AluLean” (90141902) and for Aludyne Norway for materials and casting facilities.

Compliance with Ethical Standards

Conflict of interest The authors declare that there are no personal or financial conflict of interest regarding the work in this paper.

Open Access This article is licensed under a Creative Commons Attribution 4.0 International License, which permits use, sharing, adaptation, distribution and reproduction in any medium or format, as long as you give appropriate credit to the original author(s) and the source, provide a link to the Creative Commons licence, and indicate if changes were made. The images or other third party material in this article are included in the article’s Creative Commons licence, unless indicated otherwise in a credit line to the material. If material is not included in the article’s Creative Commons licence and your intended use is not permitted by statutory regulation or exceeds the permitted use, you will need to obtain permission directly from the copyright holder. To view a copy of this licence, visit <http://creativecommons.org/licenses/by/4.0/>.

REFERENCES

1. W.-B. Lee, K.-S. Bang, S.-B. Jung, *J. Alloys Compd.* **390**, 212 (2005)
2. L.Y. Sheng, F. Yang, T.F. Xi, C. Lai, H.Q. Ye, *Compos. Part B Eng.* **42**, 1468 (2011)
3. T. Liu, Q. Wang, Y. Sui, Q. Wang, D. Wenjiang, *Mater. Des.* **89**, 1137 (2016)
4. M.R. Pinnel, H.G. Tompkins, D.E. Heath, *Appl. Surf. Sci.* **2**, 558 (1979)
5. K.J.M. Papis, J.F. Loeffler, P.J. Uggowitzzer, *Sci. China Ser. E* **52**, 46 (2009)
6. K.J.M. Papis, B. Hallstedt, J.F. Löffler, P.J. Uggowitzzer, *Acta Mater.* **56**, 3036 (2008)
7. A. Abdollah-Zadeh, T. Saeid, B. Sazgari, *J. Alloys Compd.* **460**, 535 (2008)
8. P. Xue, D.R. Ni, D. Wang, B.L. Xiao, Z.Y. Ma, *Mater. Sci. Eng. A* **528**, 4683 (2011)
9. K.S. Lee, S.E. Lee, H.K. Sung, D.H. Lee, J.S. Kim, Y.W. Chang, S. Lee, Y.N. Kwon, *Mater. Sci. Eng. A* **583**, 177 (2013)
10. M. Honarpisheh, M. Asemabadi, M. Sedighi, *Mater. Des.* **37**, 122 (2012)
11. P. Eslami, A.K. Taheri, *Mater. Lett.* **65**, 1862 (2011)
12. E. Hajjari, M. Divandari, S.H. Razavi, S.M. Emami, T. Homma, S. Kamado, *J. Mater. Sci.* **46**, 6491 (2011)
13. Y. Hu, Y.-Q. Chen, L. Li, H.-D. Hu, Z.-A. Zhu, *Trans. Nonferrous Met. Soc. China* **26**, 1555 (2016)

14. C. Nerl, M. Wimmer, H. Hoffmann, E. Kaschnitz, F. Langbein, W. Volk, J. Mater. Process. Technol. **214**, 1445 (2014)
15. T. Greß, T. Mittler, S. Schmid, P. Buchberger, W. Volk, V.G. Nardi, B. Tonn, Int. J. Metalcast. **13**, 817 (2019)
16. T. Greß, T. Mittler, S. Schmid, P. Buchberger, W. Volk, V.G. Nardi, B. Tonn, Int. J. Metalcast. (2019). <https://doi.org/10.1007/s40962-019-00387-0>
17. R.K. Tayal, V. Singh, S. Kumar, R. Gargs, Proc. Natl. Conf. Trends Adv. Mech. Eng. **212**, 1065 (2012)
18. M. Pintore, T. Mittler, W. Volk, O. Starykov, B. Tonn, Int. J. Metalcast. **12**, 79 (2018)
19. D. Chu, J.-Y. Zhang, J.-J. Yao, Y.-Q. Han, C.-J. Wu, Trans. Nonferrous Met. Soc. China **27**, 2521 (2017)
20. Y.-J. Su, X.-H. Liu, H.-Y. Huang, X.-F. Liu, J.-X. Xie, Metall. Mater. Trans. A **42A**, 4088 (2011)
21. M. Pintore, J. Wölck, T. Mittler, T. Greß, W. Volk, Int. J. Metalcast. **14**, 155 (2020)
22. W. Jiang, F. Guan, G. Li, H. Jiang, J. Zhu, Z. Fan, Mater. Manuf. Process. **34**, 1016 (2019)
23. M. Divandari, A.R.V. Golpayegani, Mater. Des. **30**, 3279 (2009)
24. G.R. Zare, M. Divandari, H. Arabi, Mater. Sci. Technol. **29**, 190 (2013)
25. S.A. Solvay, Safety Data Sheet - NOCOLOK® Cs Flux (TM) BW (2017). https://www.solvay.us/en/binaries/P36966-USA_CN_EN3-238040.pdf. Accessed 5 Feb 2018
26. J. Feng, B. Ye, L. Zuo, Q. Wang, Q. Wang, H. Jiang, W. Ding, Metall. Mater. Trans. A **48A**, 4632 (2017)
27. S. Tavassoli, M. Abbasi, R. Tahavvori, Mater. Des. **108**, 343 (2016)
28. Y. Zheng, W. Xiao, S. Ge, W. Zhao, S. Hanada, C. Ma, J. Alloys Compd. **649**, 291 (2015)
29. F.H. Samuel, J. Mater. Sci. **33**, 2283 (1998)
30. R.L. Powell, H.M. Roder, W.M. Rogers, J. Appl. Phys. **28**, 1282 (1957)
31. C.R. Ho, B. Cantor, Acta Metall. Mater. **43**, 3231 (1995)
32. G. Aylward, T. Findlay, *SI Chemical Data*, 5th edn. (Wiley, Milton, 2002)
33. J.R. Davis, in *ASM Speciality Handbook—Copper and Copper Alloys* (ASM International, Materials Park, Ohio, 2001), p. 23.
34. T. Takemoto, A. Matsunawa, T. Shibutani, Weld Int. **11**, 845 (1997)
35. J. Garcia, C. Massoulier, P. Faille, SAE Soc. Automot. Eng. **1** (2001).

Publisher's Note Springer Nature remains neutral with regard to jurisdictional claims in published maps and institutional affiliations.